International Journal of Nanoelectronics and Materials
Volume 16, No. 2, April 2023 [345-358]

Synthesis and Characterization of ZnO Nanoparticles by Pulsed Laser Ablation in Liquid Using Different Wavelengths for Antibacterial Application

Hadeel J. Imran[1], Kadhim A. Hubeatir[2*], Kadhim A. Aadim[3]

1 Laser and Optoelectronics Engineering Department, University of Technology, Iraq,
2* Laser and Optoelectronics Engineering Department, University of Technology, Iraq,
3 Department of physics, College of Science, University of Baghdad, Baghdad, Iraq,

Received 21 April 2022, Revised 28 August 2022, Accepted 27 September 2022

ABSTRACT

In this paper, the synthesis of colloidal solution of ZnO nanoparticles by PLAL using an Nd: YAG laser with 1064 nm and 532 nm wavelengths is described. The optical, morphological, structural, wettability and antibacterial activities were studied. The XRD analysis showed the hexagonal wurtzite structure while the UV-vis indicated the blue shift of the absorption peak due to the surface plasmon of the nanoparticle, which showed significant changes in color behavior. The FE-SEM revealed a uniformed spherical shape with a partial size range of 20.50–21.48 nm for ZnO at 1064 and 57.08–59.87 nm for ZnO at 532nm. Also, the concentration measurement indicated that the concentration of ZnO prepared at 1064 nm is 26.7 µg ml-1 and 63 µg ml-1 at 532 nm due to the relevance of high energy to the Zn plate and little distortion in the water and high absorption of short wavelength. Finally, the optical density of the antibacterial activity has been investigated, and both concentrations have good antibacterial activity at 12 h. The ZnO prepared at 532 nm has higher antibacterial activity because it has a high concentration of nanoparticles for both S. aureus and E. coli. Finally, the cell viability for ZnO synthesis with both 1064 nm and 532 nm indicates that this material has high biocompatibility and could be used for medical applications.

Keywords: Antibacterials, Nanoparticles, PLAL, Zinc oxide.

1. INTRODUCTION

The technique of Pulsed Laser Ablation in Liquids (PLAL) is one of the most simple and versatile methods for nanostructured materials fabrication with different types. PLAL has numerous advantages over conventional approaches. The procedure is flexible, and the chemical reagent presence in the solution [1]. There are many parameter effects on the size, structure, morphology of nano-particle material synthesized by PLAL, such as solvent type, surfactant molecules' existence, laser energy, laser wavelength, and ablation time [2]. The ablation process begins with focusing the laser beam on a substrate surface with high intensity inside the liquid medium. The plasma plume was generated due to the laser-matter interaction with the surface, removing the particles from the

*Corresponding author: Kadhim.A.Hubeatir@uotechnology.edu.iq

solid target surface. This condition results in the formation of special thermodynamic conditions with higher temperature and pressure, allowing the production of tiny particles in the nanoscale range [1], [3].

Nanostructured materials have garnered considerable attention in the previous years due to the potential properties they have gained and developed that enable them to be applied in a variety of application fields, including electrical, magnetism, optics, biology, and electronics [4]–[7]. These properties have been used to solve different problems in science and technology through the novel behavior of nanostructured materials. As a result, these materials have been discovered in a variety of significant scientific and technological fields, allowing for the development of new applications [8]. Many chemical or physical methods, such as chemical precipitation, are used to make particles that are the right size for a project [9], sol-gel [10], and chemical vapor deposition [11]. As a result, many research groups have exhaustively researched each approach to find and quantify the effect parameters that can be utilized to modify the particle size in the nanoscale region. Furthermore, they spent a significant amount of time and effort determining the effectiveness of these factors in generating nanostructures with good distribution and reproducibility in a range of materials [3].

A correlation has been found between the antibacterial beaver of metal nanoparticles and size of the particles and the surface-to-volume ratio of the particles, due to the release ions of metal through solutions, this encourages the researcher to deal directly with membranes of microbial rather than simply observing them [12]. Zinc oxide nanoparticles (ZnO NPs) have generated significant attention due to their intriguing physicochemical characteristics [12]. It is essential in science and technology applications such as nonlinear optics, electronic devices, catalysis, and medical applications, and in the development of promising antimicrobial agents [13]. Because of their efficacy against pathogen-resistant strains, low toxicity, and heat resistance, ZnO NPs have been utilized as antimicrobial agents [1].

Suha I. Al-Nassar et al. used liquid phase pulsed laser ablation to examine the impact of laser pulses energy on the formation of ZnO NPs. They found that by increasing the pulse energy for preparation of the ZnO NPs led to an increase in the size and concentration of particles in the colloidal [14]. Khawla S. Khashan et al. synthesized and characterized zinc oxide nanostructured materials using the laser ablation method. Their findings indicate that *Staphylococcus aureus* (*S. aureus*) has a larger inhibition zone than *Escherichia coli* (*E.coli*) [15]. Ayman M. Mostafa et al. synthesized ZnO and core/shell Au@ZnO nanocatalysts in a variety of liquid media using pulsed laser ablation. They found that increasing the pulse energy for preparation of the ZnO NPs led to an increase in the size and concentration of particles in the colloidal. They conclude that ZnO NPs could break down the 4-nitrophenol about 90% in 12 minutes, but the Au@ZnO can do the same thing in just 4 minutes [16].

In this work, ZnO NPss have been synthesized using the laser ablation method with different wavelengths (1064 and 532 nm) to enhance their antibacterial activity at room temperature. The structure, optical, and morphological characteristics of ZnO thin film have been analyzed by different techniques: UV-Vis spectrophotometer, X-ray diffraction, Field Emission Scanning Electron Microscope, and Energy-dispersive X-ray spectroscopy The antibacterial activity of synthesized samples was investigated for *E. coli* and *S. aureus*. Also, the cell viability inside the nanoparticles has been examined using MTT analysis (3-(4,5-dimethylthiazol-2-yl)-2,5-diphenyltetrazolium bromide), which also gave an indication of the toxicity of the NPs.

2. EXPERIMENTAL WORK

2.1 Preparation of ZnO NPs

A zinc plate has a 1 × 1 cm surface area and a high purity (99.98%). All of the samples were dissolved in distilled water, which served as a common solvent. PLAL has been used to synthesize ZnO NPs. When the pellet is immersed in deionized water, it is filled with 3 ml and the water level above the target is adjusted to be approximately 10 mm above the surface of the target. It was decided to use Nd: YAG lasers with wavelengths of 1064 and 532 nm for the laser ablation process, and the laser energy used for the ablation was 200 mJ with a repetition frequency of 7 Hz for a total of 10 minutes. In this experiment, a positive lens with a focal length of 9 cm was used to focus the laser beam on the ZnO pellet, resulting in a 2.5 mm area around the pellet. Figure 1 depicts a schematic diagram of the project's organization.

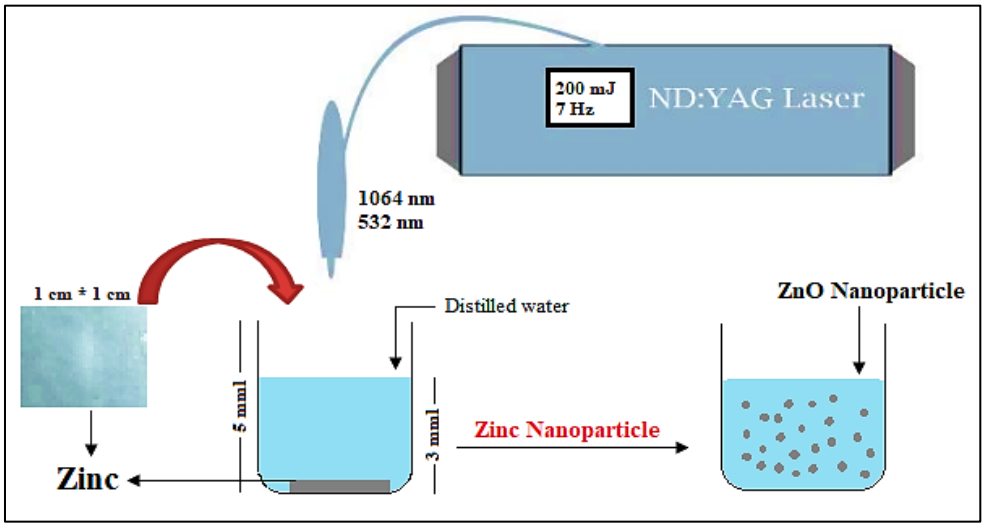

Figure 1: The schematic diagram of experimental work.

2.2 Characterization of ZnO NPs

The crystal structure of the synthesized ZnO NP was performed through the use of an X-ray diffraction (XRD) technique with the Cu-K target from PANalytical X Pert Pro (λ = 0.1540 nm). For optical property measurement, the UV–Vis spectrophotometer model (Metertech, SP8001 spectrophotometer, Japan) in the range of 100–900 nm was used. The concentration of nanoparticles in the colloidal was measured using Atomic Absorption Spectrometry (AAS). Field emission scan electron microscopy (FE-SEM) has been used to examine the surface morphology, particle size, and chemical composition of prepared nanoparticles, which was done with a JSM-IT800 (origin) equipped with an energy dispersive X-ray EDX.

2.3 Cell Viability of ZnO NPs

The cell viability test was investigated using human white blood cells (the blood was collected from healthy volunteers at 25 years of age) under highly sterile conditions. The white blood cells with a

density of 1×10^4 cells/ml in the well plate were exposed to the NPs then incubation at 37 °C for 24 hours. Thereafter, the plate contained was poured out and washed with phosphate-buffered saline three times to remove any trace of nano particles, then 10 µl of MTT dye solution has been added to the well plates and incubated for four hours at 37 °C. Then the cells were washed several times with PBS until the excess dye was removed. After the plates were completely dry, the results were read with the ELISA microplate spectrophotometer at a wavelength of (500) nanometers.

2.4 Antibacterial Activity of ZnO NPs

E. coli and *S. aureus* were used to test the antibacterial properties of the NPs. A sterile wire loop was used to separate the bacteria from their stock cultures [17]. To assess how NPs affect the growth curve of bacteria, M-H agar plates were used to culture the bacterial strains at 37 °C. A nutrient broth solution of 50 ml was used to prepare the collection of freshly cultured plates. Bacteria multiplied until an optical density (OD) of 0.1 at 600 nm was achieved in the nutrient broth, corresponding to a bacterial concentration of 108 CFU/ml in the presence of the light source. Then, 1 ml of bacterial cultures was added to the NP-supplemented nutrient broth, and the mixture was incubated for 12 hours at 37 °C with only slight stirring. The optical density (OD) of the bacteria was measured using a spectrophotometer to determine their growth [18], [19].

3. RESULTS AND DISCUSSION

In the distilled water environment, intense laser pulses interact with the solid zinc target, causing target ablation and the expansion of the plasma plume. The liquid prevents plume expansion, as evidenced by the liquid splashing during the process, resulting in high pressure and temperature. The technique of PLAL was successfully produced ZnO as shown in Figure 2. The color of ZnO NPs colloid turned yellowish by using 1064 nm wavelength and become darker into brownish when using 532 nm wavelength because of higher concentration. Since at wavelength of 532 nm was less affected by water and has more energy than 1064 nm wavelength, so it ablates more particle from the target surface. The most important reason for this concentration difference is for a shorter wavelength, the larger optical absorption will take place [20]. The concentration of the prepared nanoparticles was measured by using Atomic Absorption Spectrometry (AAS). The experimental parameter and concentration result of each sample were listed in Table 1.

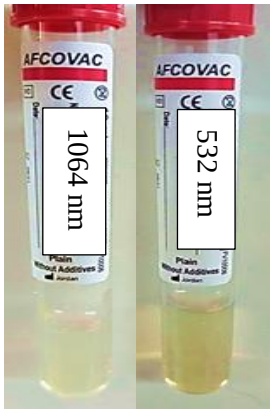

Figure 2: Colloidal suspension of ZnO nanoparticle prepared by PLAL technique.

Table 1: The experimental parameter of the prepared ZnO and the concentration of nanoparticles.

Name	Power (mJ)	Wavelength (nm)	Concentration (μg ml^{-1})
ZnO	200	1064	26.7
ZnO	200	532	63

3.1 X-ray Diffraction (XRD)

The structure and degree of crystallinity of ZnO NPs synthesized were investigated using XRD. Figure 3 shows the XRD pattern of ZnO NPs prepared at wavelengths of 1064 and 532 nm. For 532 nm wavelength, the XRD peak is located at 2θ = 34.23, 36.38, and 43.93 ° indexed as (002), (101), and (200). On the other hand, the ZnO film prepared at 1064 nm wavelength, the observed peak is 2θ = 34.6, 36.6, 36.2, and 43.8 ° indexed as (002), (101), and (200). These patterns are in a good agreement with standard care (96-230-0451). This result indicates that the film has a polycrystalline nature and has a hexagonal wurtzite structure. It could be noticed that there are a different in the high of the peaks, where the pack of sample prepared at wavelength of 532 nm was higher than that prepared at 1064 nm wavelength because it has high concentration of ZnO NPs so that there are more particle oriented in a hexagonal wurtzite structure. Table 2 indicate the lattice parameter, full width half maximum, and the average crystal size, D, of the sample was measured using Debye– Scherrer equation:

$$D = (k\lambda)/(\beta \cos\alpha) \qquad (1)$$

Where k is 0.9 the Scherrer constant, λ is the X-ray constant (0.15406 nm), , β is the fill width half maximum (FWHM) and α is Braggs angle [21].

Figure 3: The XRD patterns of each ZnO colloidal prepared via PLAL.

The XRD information for both samples were listed in Table 2 which include the 2θ, FWHM, Crystalline size (nm), hkl, average crystal size and card number. According to the table and equation (1) the FWHM was inversely proportional with crystal size. Also, it was noticeable that there are decreasing in FWHM in sample prepared at wavelength of 532 nm with increasing the peak intensity and crystal size which mean crystallinity improvement as the ZnO concentration increase in the colloidal. This result is in accordance with previous research [22]. So that, the highest crystallinity was obtained in the ZnO NP prepared with 532 nm wavelength which has large crystal size and lower FWHM.

Table 2: The lattice parameter of ZnO crystal.

Wavelength(nm)	2θ (°)	FWHM (Degree)	Crystalline size (nm)	(hkl)	Average C.S (nm)	Card No.
532	34.23	0.2	41.657	002	57.689	96-230-0451
	36.38	0.1	83.782	101		96-230-0451
	43.93	0.18	47.629	200		96-230-0451
1064	34.6	0.6	13.872	002	18.099	96-230-0451
	36.6	0.4	20.932	101		96-230-0451
	43.8	0.44	19.493	200		96-230-0451

3.2 Ultraviolet-Visible (UV-Vis) Analysis

The optical absorption spectra for synthesized ZnO (at wavelengths of 532 nm and 1064 nm) which were prepared via laser ablation are shown in Figure 4. The absorption spectra have a peak at 221 nm and 224 nm for wavelengths of 1064 nm and 532 nm, respectively. These absorption peaks indicate the production of nanoparticles inside the solution. The absorption band of the solution moves toward shorter wavelengths (blue shift) at both wavelengths, but the peak was higher at 532 nm wavelength, which means more nanoparticle formation. Shifting toward shorter wavelengths indicates the formation of smaller nanoparticles as a result of the quantum confinement effect. The absorption values are determined by the concentration of nanoparticles produced; a higher concentration produces a larger absorption peak. Results show that at wavelength of 532 nm, the absorption peak amplitude was greater than expected on the zinc plate because the solution contained a higher concentration of the produced nanoparticles where more particle concentration means more absorption.

Furthermore, the energy band gap for the prepared sample was calculated from the extrapolation of hυ vs $(\alpha h\upsilon)^2$ curve. Where hυ denotes the discrete energy bandgap of the light, α denotes the absorption, A denotes a constant that depends on the length of the localized state tails, and Eg denotes the optical energy bandgap. The band gap value was obtained by drawing a straight line on the curve which was intersected with hυ at the X-axis. Figure 5 shows the band gap of prepared ZnO, which exhibits higher band gap energy. As expected, the smaller partial size has a higher band gap, where it was 4.25 eV at 532 nm wavelength, and 4.4 eV at 1064 nm wavelength. This indicates that the

particle formed at wavelength of 1064 nm was smaller than that formed at wavelength of 532 nm. This result is consistent with Ref. [14].

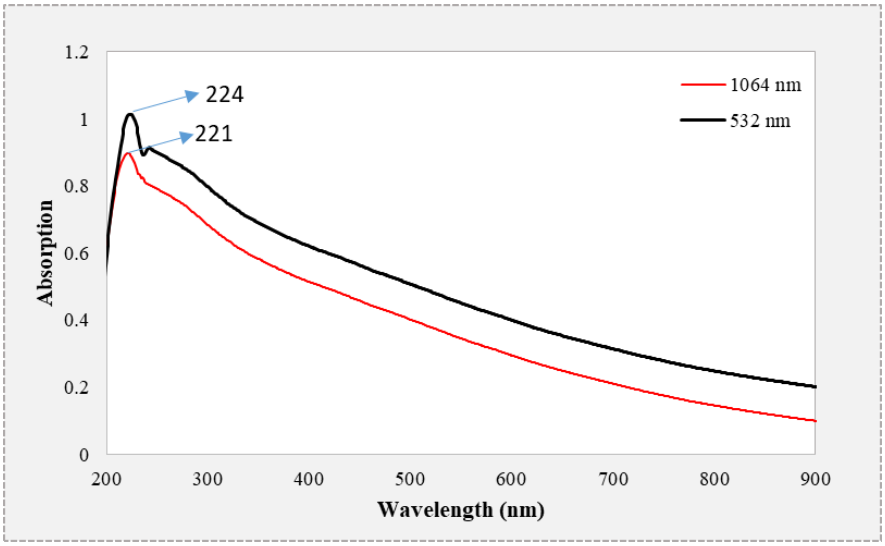

Figure 4: UV-vis absorption spectrum of the ZnO nanoparticle prepared by PLAL.

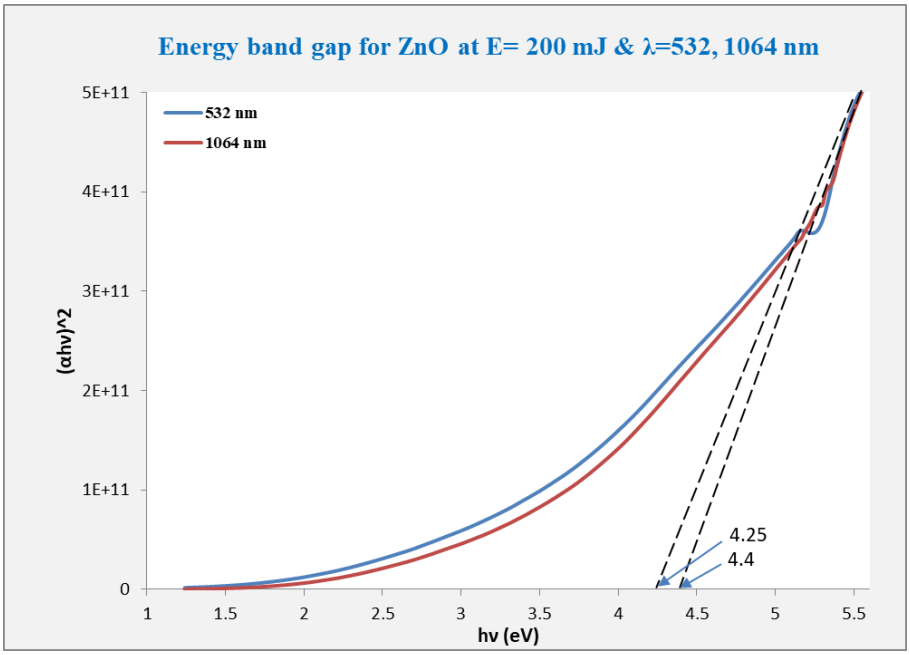

Figure 5. Energy band gap determination for ZnO nanoparticle.

3.3 Field Emission Scan Electron Microscopy (FE-SEM)

The ZnO NPs were analyzed using Field Emission Scan Electron Microscopy (FE-SEM), which was supplemented by EDX to establish the morphological structure, grain size, shape, and to obtain the chemical composition. Figures 6(a) and (b) show that the surface was covered by uniform and small particle, and Figure 6(c) displays the histogram graph for the particle distribution which shows that nanoparticles synthesize about 10-22 nm at 1064 nm wavelength and the maximum particle was approximately 16 nm. While at 532 nm wavelength, the synthesized nanoparticle the grain had 20-70 nm in size, it was also uniform but had a little aggregation as shown in Figure 7. The reason for the particle size being bigger at 532 nm wavelength are due to high concentration of ZnO nm??. As a result the absorption of water at wavelength of 1064 nm was more than at 532 nm wavelength, which led to a decrease in the energy reached to the pellet surface and ablation of a small particle in size and concentration (26.7 μg ml−1), while no water absorption at 532 nm wavelength. This means all the energy from the laser pulses goes to the pellet, leading to large particle ablation with concentration (63 μg ml−1). Also as mentioned before the shorter wavelength was highly absorbed by the material. Each wavelength for the preparation of nanoparticles has shown a well-defined particle like morphology with a plenitude of spherical shape particles, which was more preferred for antibacterial application.

The EDX result showed that the thin film contained oxygen and zinc, which means that the film was ZnO. Also, the EDX result proved that at 532 nm wavelength, the concentration of ZnO is higher than at 1064 nm wavelength because of the same result as written above in FE-SEM. All the other elements emitted in the EDX figure are for the substrate, which is glass. The EDX result is shown in Figures 8(a) and (b).

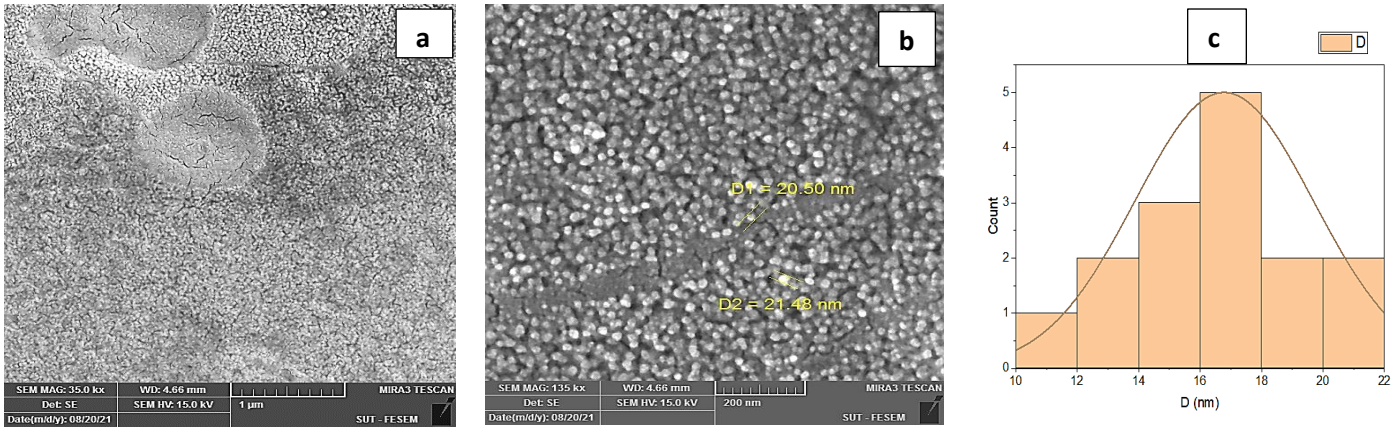

Figure 6: FE-SEM image of ZnO film prepared by 1064 nm laser wavelength.

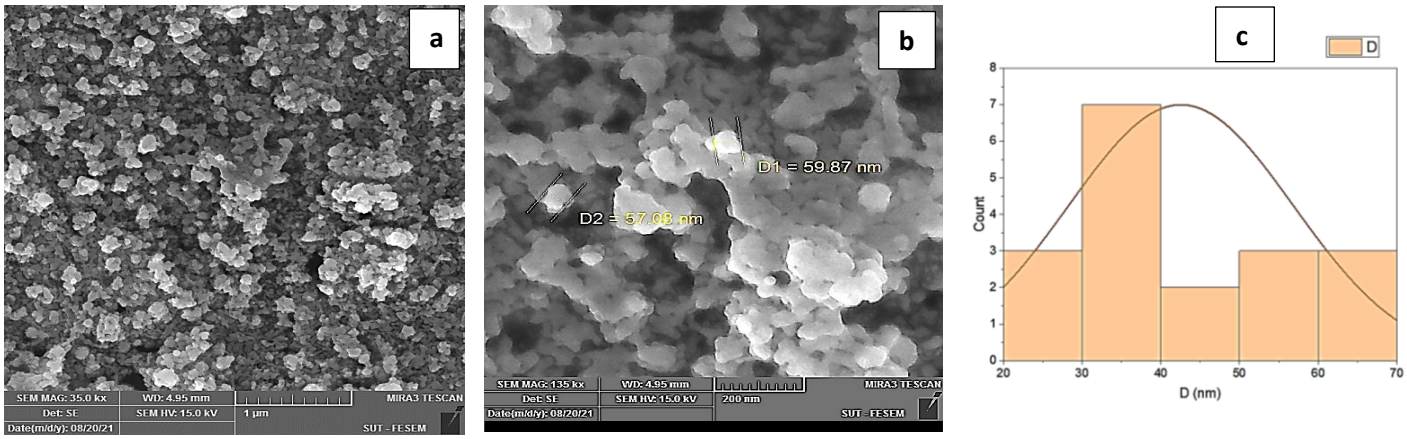

Figure 7: FE-SEM image of ZnO film prepared by 532 nm laser wavelength.

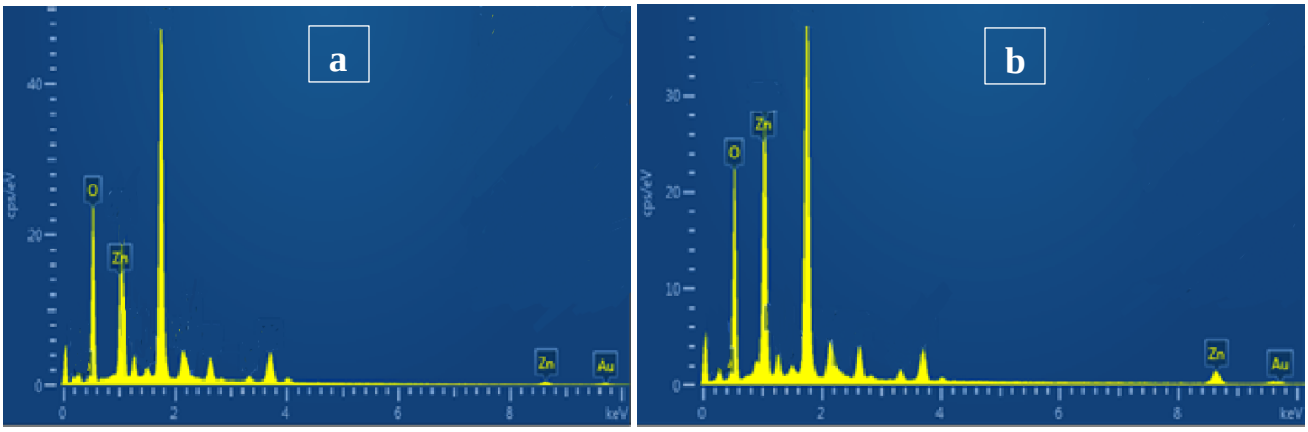

Figure 8: The EDX result of ZnO nanoparticle (a) prepared at wavelength of 1064 nm, (b) prepared at wavelength of 532 nm.

3.4 Contact Angle

In vitro wettability of biomaterials is assessed using the contact angle (CA) at the liquid-solid interface. A high CA or high fluid-solid adhesion indicates a hydrophobic solid surface or low wettability. A low CA indicates a high wettability or hydrophilic surface, which means a continuous fluid film over the solid surface. Three forces influence the wettability of a solid substrate: the surface tension of the solid, the surface tension of the liquid, and the interfacial tension [23]. Figure 9 shows the prepared colloidal's contact angle, which seems to be between 26.67 ° and 27.89 ° for ZnO synthesized at wavelength of 1064 nm and between 22.78 ° and 22.71 ° for ZnO synthesized at 532 nm wavelength. This means that the nanoparticle in colloidal has less interfacial tension which decreases the CA and increases the wettability among the surface. So the higher concentration has lower CA and higher wettability. The CA of the two samples was an indication that the material has high biocompatibility because it has high wettability which was one of the most important

biomaterial characteristics. Finally, the higher wettability means larger area covered with colloidal and this means high antibacterial effect.

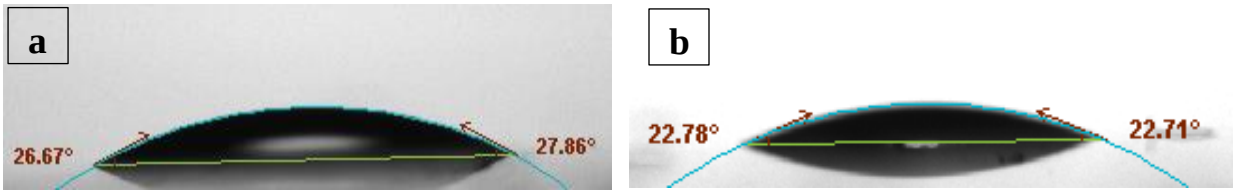

Figure 9: Contact angle image of the prepared ZnO at wavelength of (a) 1064 nm, (b) 532 nm.

3.5 Antimicrobial OD Test

The OD600 of bacteria treated with synthesized nanomaterial was measured to perform the antibacterial activity quantitatively. Figure 10 depicts the growth curves of *Staphylococcus aureus* (a gram-positive bacterium) and *Escherichia coli* (a gram-negative bacterium) after ZnO treatment (prepared at wavelengths of 1064 nm and 532 nm). In this work, the used antibacterial concentrations for *S. aureus* and *E. coli* were 26.7 and 63 g ml1 for ZnO NPs prepared at wavelength of 1064 and 532 nm, respectively. Both concentrations have good antibacterial activity at 12 hours??, as shown by the curves. Furthermore, the highest concentration from ZnO NPs applied on both bacteria showed the greatest antibacterial activity. In the case of *E. coli*, the bacteria's inhibition levels were not significantly different from one another when compared to *S. aureus*. In comparison of the bacterial growth curve with that of the control curve, ZnO has greater bacterial inhibition against *S. aureus* than *E. coli*, and the inhibition increases with increasing nanoparticle concentration. The findings revealed that the ZnO nanomaterial had significant antibacterial activity against both gram-positive and gram-negative bacteria.

This study demonstrates that ZnO NPs have effective antibacterial activity when prepared with both wavelengths (1064 nm and 532 nm) at very low concentrations for short periods of time. Also, for both bacteria, the ZnO prepared at 532 nm wavelength has higher antibacterial activity because it has a high concentration of nanoparticles, where the concentration plays quite an important role in the growth of bacteria. These finding was agreed with Sathyanarayanan et al. [24].

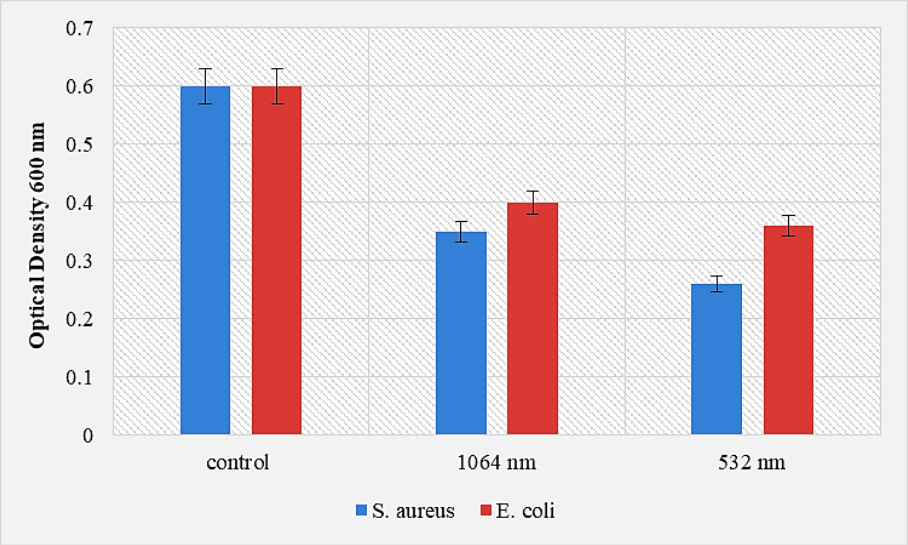

Figure 10: Effect of ZnO NPs in *S. aureus* growth curve and *E. coli* growth curve.

3.6 Cell Viability

The effect of the nanoparticles on the cell viability of white blood cells has been measured using an ELISA micro plate spectrophotometer. The nanomaterial activity against the biological system and cells is one of the most significant factors for biomaterial requirements, which makes them suggested for medical application. Thus, the response of the white blood cells to ZnO NPs synthesis at both 1064 nm and 532 nm wavelength was investigated via an MTT assay after 24 hours of exposure to NPs. From Figure 11, it could be demonstrated that the minimum viability is 79.29% for ZnO synthesized at 1064 nm wavelength and a maximum of 87.51% for ZnO synthesized at 532 nm wavelength because the particle size of synthesized at 1064 nm wavelength was smaller than that of synthesized at 532 nm wavelength, where the smaller size has the most effect on the cell. So that the colloidal synthesized with 532 nm wavelength has higher cell viability and higher antibacterial result which made them batter biomaterial. However, both samples have high cell viability present in general therefore, the ZnO NPs synthesized in both wavelength indicate high biocompatibility.

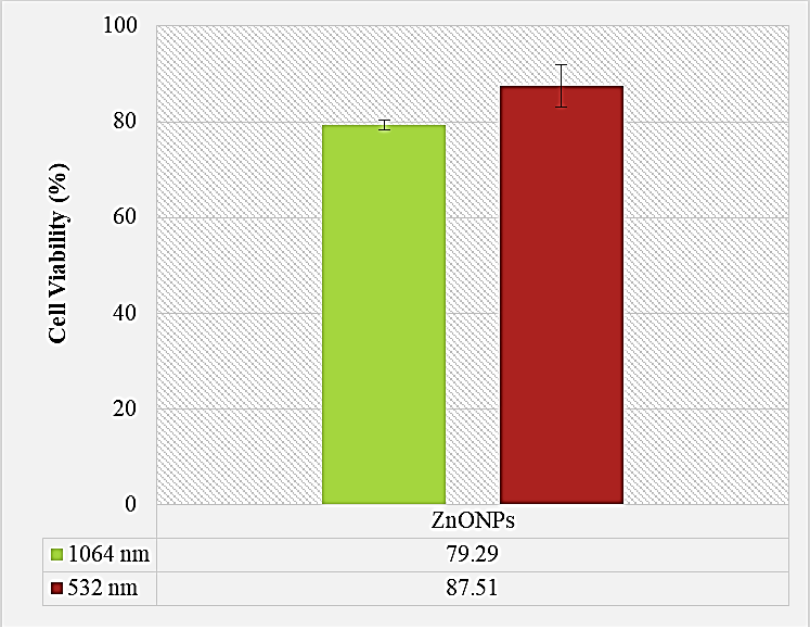

Figure 11: The white blood cells viability of ZnO NPs.

4. CONCLUSION

The ZnO nanoparticle was successfully synthesized by using the solid stat Nd: YAG laser at 1064 nm and 532 nm wavelength using the PLAL technique. We concluded that the NP prepared using 532 nm have larger size than 1064 nm and it was in XRD result and FESEM result. Where the shorter wavelength, the more absorption and high concentration and larger size. As well as the prepared NP was good biocompatibility because of lower contact angle indicates that each sample has excellent wettability. Also the papered NP success in work as antibacterial and the antibacterial test demonstrates that the ZnO effect is well proven when prepared with both wavelengths at very low concentrations in a short time. Also, for both bacteria, the ZnO prepared at 532 nm has higher antibacterial activity because it has a high concentration of nanoparticles. Finally, the cell viability for ZnO synthesis with both 1064 nm and 532 nm indicate that this material have high biocompatibility and could be used for medical applications.

ACKNOWLEDGEMENT

This work was supported by the University of Technology, Iraq. We would also like to acknowledge the University of Baghdad for supplying the necessary equipment and devices for this study.

REFERENCES

[1] Menazea, A. A., J. Mater. Res. Technol., vol **9**, issn 4 (2020) pp. 1–7.
[2] Ma, R., Reddy, D. A., and Kim, T. K., Bull. Korean Chem. Soc., vol **36,** no. 1 (2015) pp. 5–6.
[3] Mostafa, A. M. and Mwafy, E. A., Environ. Nanotechnology, Monit. Manag., vol **14**, (2020) p. 100382.
[4] Imran, H. J., Hubeatir, K. A., Aadim, K. A., and Abd, D. S., "Preparation Methods and Classification Study of Nanomaterial: A Review," in Iraqi Academics Syndicate International Conference for Pure and Applied Sciences (IICPS), vol. 1818, (2021) p. 12127.

[5] Nayef, U. M., Hubeatir, K. A., and Abdulkareem, Z. J., Mater. Technol., vol **31,** no. 14 (2016) pp. 884–889.
[6] Nayef, U. M., Hubeatir, K. A., and Abdulkareem, Z. J., "Ultraviolet photodetector based on TiO2 nanoparticles/porous silicon hetrojunction," Optik (Stuttg)., vol. 127, no. 5 (2016) pp. 2806–2810.
[7] Aadim, K. A., Jassem, R. H., Adil, B. H., Farhan, M. M., and Al-Chalabi, S. M., "Synthesis of zinc nanoparticles by laser induced plasma and its effects on levels of thyroid hormones," AIP Conf. Proc., vol. 2307 (2020) pp. 1-7.
[8] Eisa, W. H., Zayed, M. F., Anis, B., M.Abbas, L., Ali, S. M., and Mostafa, A. M., J. Clean. Prod., vol **241,** (2019) p. 118398.
[9] Zhou, S. Y., Wu, L., Li, D., Li, X., Huo, J., Wang, P., Yan, H. Y., J. Alloy. Compd., vol **817,** (2020) p. 152707.
[10] Itteboina, R. and Sau, K. T., "Sol-gel synthesis and characterizations of morphology-controlled Co3O4 particles," in International Conference on Nanoscience and Nanotechnology (ICNAN'16), vol 9, (2019) pp. 458–467.
[11] Mwafy, E. A., Dawy, M., Abouelsayed, A., Elsabbagh, I., and Elfass, M., Res. J. Pharm. Biol. Chem. Sci., vol **8,** (2017) pp. 375–382.
[12] Gupta, V. K., Fakhri, A., Tahami, S., and Agarwal, S., J. Colloid Interface Sci., vol **504,** (2017) pp. 164–170.
[13] Hubeatir, K. A., Laser, Eng. Technol. J., vol **34,** (2016) pp. 178–185.
[14] Al-Nassar, S. I., Hussein, F. I., and Ma, A. K., J. Mater. Res. Technol., vol **8,** no. 5 (2019) pp. 4026–4031.
[15] Khashan, K. S., Badr, B. A., Sulaiman, G. M., Jabir, M. S., and Hussain, S. A., "Antibacterial activity of Zinc Oxide nanostructured materials synthesis by laser ablation method," in Journal of Physics: Conference Series, vol 1795, no. 1 (2021) pp. 1–5.
[16] Mostafa, A. M. and Mwafy, E. A., J. Mater. Res. Technol., vol **9,** no. 3 (2020) pp. 3241–3248.
[17] Jabir, M. S., Nayef, U. M., Jawad, K. H., Taqi, Z. J., Buthenhia, H., and Ahmed, N. R., "Porous silicon nanoparticles prepared via an improved method: A developing strategy for a successful antimicrobial agent against Escherichia coli and Staphylococcus aureus," in International Conference on Materials Engineering and Science, vol 454, no. 1 (2018) pp. 1–9.
[18] Bahjat, H. H., Ismail, R. A., Sulaiman, G. M., and Jabir, M. S., J. Inorg. Organomet. Polym. Mater., vol **31,** no. 9 (2021) pp. 3649–3656.
[19] Bhaisare, M. L., Wu, B. S., Wu, M. C., Khan, M. S., Tseng, M. H., and Wu, H. F., Biomater. Sci., vol **4,** no. 1 (2016) pp. 183–194.
[20] Idris, S. N., Norizan, M. N., Mohamad, I. S., Mahmed, N., Magiswaran, K., and Sobri, S. A., Int. J. Nanoelectron. Mater., vol **14,** no. Special Issue InCAPE (2021) pp. 199–206.
[21] Rini, A. S., Rati, Y., Umar, A. A, and Abdullah, N. A., Int. J. Nanoelectron. Mater., vol **13,** (2020) pp. 21–32.
[22] Özdal, T., Taktakoɩlu, R., Özdamar, H., Esen, M., Takçi, D. K., and Kavak, H., Thin Solid Films, vol **592**, (2015) pp. 143–149.
[23] Menzies, K. L. and Jones, L., Optom. Vis. Sci., vol **87,** no. 6 (2010) pp. 387–399.
[24] Sathyanarayanan, M. B., Balachandranath, R., Genji Srinivasulu, Y., Kannaiyan, S. K., and Subbiahdoss, G., ISRN Microbiol., vol **2013** (2013) pp. 1–5.